Vol. 39, No. 1 (2017) 31-44

Tribology in Industry

www.tribology.fink.rs

RESEARCH

Effect of Magnetohydrodynamic Couple Stresses on Dynamic Characteristics of Exponential Slider Bearing

N.B. Naduvinamani[a], A. Siddangouda[b], P. Siddharam[c]

[a] *Department of Mathematics , Gulbarga Univesity,Kalaburagi-585106, Karnataka, India,*
[b] *Department of Mathematics, Appa Institute of Engineering & Technology,Kalaburagi-585103 India,*
[c] *Department of Science, Government Polytechnic, Shorapur-585224, India.*

Keywords:

Couple stress
MHD
Reynolds Equation
Dynamic stiffness
Dynamic Damping

Corresponding author:

N.B. Naduvinamani
Department of Mathematics,
Gulbarga Univesity,Kalaburagi, India.
Email:naduvinamaninb@yahoo.co.in

A B S T R A C T

The effect of couple stresses on static and dynamic characteristics of exponential slider bearing in the presence of magnetic field considering squeeze action is theoretically analyzed in this paper. The modified magnetohydrodynamic couple stress Reynolds type equation is derived on the basis of Stokes couple stress model and closed form expressions are obtained for static and dynamic character coefficients. Comparing with bearing lubricated with non-conducting Newtonian lubricants, the magnetohydrodynamic couple stress lubrication provides the higher steady load carrying capacity, dynamic stiffness and damping coefficient. The exponential bearing shows higher efficiency for small film thickness at higher value of couple stress parameter and Hartmann number.

1. INTRODUCTION

Magnetohydrodynamics (MHD) is the study of dynamics of the flow of electrically conducting fluid in presence of a magnetic field. Many researchers investigated the effects of MHD on the characteristics of bearings such as slider bearing by Snyder [1], inclined slider bearing and finite step slider bearing by Hughes [2,3], parallel plate slider bearing and journal bearing by Kuzma [4,5] and finite rectangular plates by Lin [6]. These studies concluded that the application of magnetic field improves on bearings performance. All these studies are on classical hydrodynamic lubrication and lubricant assumed is to be Newtonian fluid which is not satisfactory assumption for practical application in engineering field. Owing to importance of Newtonian lubricants blended with microstructure additives many theories were developed to describe these fluids. The simplest theory among these was developed by Stokes [7]. The Stokes theory allows for polar effects such as the presence of couple stresses, body couples and non-symmetric stress tensors. On the basis of Stokes theory, many researchers studied effect of couple stress on bearing characteristics such as slider bearing by Ramanaiah and Sarkar [8], short journal bearing by Ayyappa et al. [9], circular stepped plates by Naduvinamani and Siddangouda [10] and long partial journal bearing by Lin [11]. According to the results obtained, the use of non-Newtonian fluid enhances the bearing performance

characteristics. Siddangouda [12] studied the effect of non-Newtonian micropolar fluid on the characteristics of parallel stepped plates.

On the basis of results obtained in the studies of MHD effect and couple stress effect, the researchers are devoted towards the study of bearing performance with the combined effect of MHD and couple stress. The combined effects of couple stress and MHD on bearing characteristics are studied by Das [13], circular stepped plates by Naduvinamani et al. [14] and different types of finite plates by Fathima et al. [15]. The results obtained in these studies showed an increase in load carrying capacity of bearings as the strength of applied magnetic field increases and also with increase in the value of couple stress parameter. The study of static and dynamic characteristics of bearing plays an important role in the consideration of geometry of bearing. Basic reference for bearing design is provided by the static characteristics and stability behaviour of bearing is predicted by the dynamic characteristics. Effect of non-Newtonian fluid on Static characteristics of Journal bearings are studied by Javorova et al. [16] and pivoted curve bearing by Singh et al. [17]. Dynamic characteristics of plane inclined slider bearing in the presence of magnetic field are studied by Lin et al. [18] and it is concluded that applied magnetic field enhances the dynamic characteristics of bearings. Lin and Hung [19] studied the dynamic characteristics of exponential bearing. The effect of MHD on dynamic characteristics of exponential slider bearings is studied by Lin and Lu [20]. Recently static and dynamic characteristics of MHD couple stress plane and parabolic slider bearings is studied by Naduvinamani et al. [21].

In the present paper, the effect of couple stress on static and dynamic characteristics of exponential slider bearing in the presence of applied magnetic field is analyzed. The results obtained are compared with that of non-magnetic case by Lin and Hung [19] and the Newtonian case obtained by Lin and Lu [20].

2. MATHEMATICAL FORMULATION

The geometry of exponential slider bearing of length L is shown in Fig. 1. Conducting couple stress fluid is considered in the film region. The lower bearing surface is moving with a velocity U in the x-direction and the upper surface ($y = h$) has a squeezing effect $\partial h/\partial t$. In the direction perpendicular to the bearing, a uniform transverse magnetic field B_0 is applied. The following realistic assumptions are made in the simplification of constitutive equations:

1. The fluid film is thin.
2. Inertial forces are negligible in comparison with viscous forces.
3. The body couples and body forces are negligible except Lorentz force.
4. Induced magnetic field is small as compared to externally applied magnetic field.
5. The bearing surfaces are perfect insulators and there is no external circuit in the fluid.

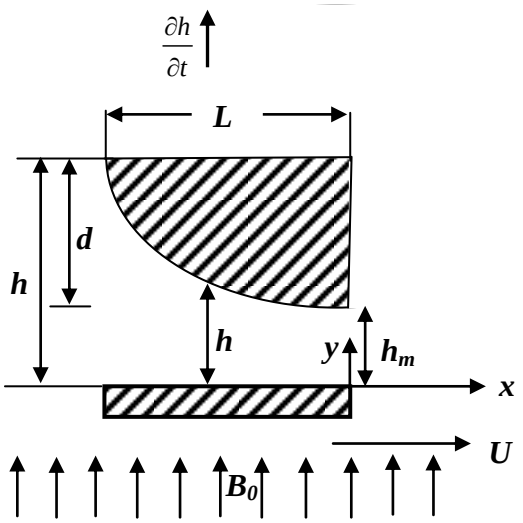

Fig. 1. Geometry of exponential slider bearing.

Under these assumptions, the constitutive equations for couple stress fluid in the presence of applied magnetic field reduce to (Das[13]):

$$\mu\frac{\partial^2 u}{\partial y^2}-\eta\frac{\partial^4 u}{\partial y^4}-\sigma {B_0}^2 u=\frac{\partial p}{\partial x}+\sigma E_z B_0 \tag{1}$$

$$\frac{\partial p}{\partial y}=0 \tag{2}$$

$$\frac{\partial u}{\partial x}+\frac{\partial v}{\partial y}=0 \tag{3}$$

$$\int_{y=0}^{h}\left(E_z+B_0 u\right)dy=0 \tag{4}$$

where μ is the lubricant viscosity; η is material constant responsible for couple stresses; σ is the conductivity of the lubricant; p is the film pressure; and u, v are the velocity components in

the x and y directions respectively; E_z is the component of electric field in z-direction. The relevant boundary conditions for velocity components are:

$$\text{At } y=h; \quad u=0, \quad \frac{\partial^2 u}{\partial y^2}=0, \quad v=\frac{\partial h}{\partial t}; \tag{5}$$

$$\text{At } y=0; \quad u=U, \quad \frac{\partial^2 u}{\partial y^2}=0, \quad v=0; \tag{6}$$

3. SOLUTION OF THE PROBLEM

The solution of equation (1) subject to the boundary conditions given by equations (5) and (6) under condition (4) is obtained as:

$$u=-\frac{U}{2}\lambda_1-\frac{{h_{ms}}^2 h}{2l\mu M^2}\frac{\partial p}{\partial x}\lambda_2 \tag{7}$$

where,

$$\lambda_1=\lambda_{11}-\lambda_{12}, \lambda_2=\lambda_{13}-\lambda_{14} \quad \text{for } \frac{4M^2l^2}{{h_{ms}}^2}<1 \tag{8a}$$

$$\lambda_1=\lambda_{21}-\lambda_{22}, \lambda_2=\lambda_{23}-\lambda_{24} \quad \text{for } \frac{4M^2l^2}{{h_{ms}}^2}=1 \tag{8b}$$

$$\lambda_1=\lambda_{31}-\lambda_{32}, \lambda_2=\lambda_{33}-\lambda_{34} \quad \text{for } \frac{4M^2l^2}{{h_{ms}}^2}>1 \tag{8c}$$

where $M=B_0 h_{ms}\left(\sigma/\mu\right)^{1/2}$ is the Hartmann number and $l=\left(\eta/\mu\right)^{1/2}$ is the couple stress parameter. The relations in above expressions are provided in Appendix-A.

With the use of boundary conditions (5), (6) and the expression (7) for u, the integration of continuity equation (3) over the film thickness gives the modified Reynolds equation in the form:

$$\frac{\partial}{\partial x}\left\{G\left(h,l,M\right)\frac{\partial p}{\partial x}\right\}=6\mu U\frac{\partial h}{\partial x}+12\mu\frac{\partial h}{\partial t} \tag{9}$$

where, $G(h,l,M)$

$$=\begin{cases}\dfrac{6{h_{ms}}^2h^2}{lM^2}\left\{\dfrac{\alpha^2-\beta^2}{\dfrac{\alpha^2}{\beta}\tanh\left(\dfrac{\beta h}{2l}\right)-\dfrac{\beta^2}{\alpha}\tanh\left(\dfrac{\alpha h}{2l}\right)}-\dfrac{2l}{h}\right\} & \text{for } \dfrac{4M^2l^2}{{h_{ms}}^2}<1\\ \dfrac{6{h_{ms}}^2h^2}{\mu lM^2}\left\{\dfrac{2\left(\cosh\left(\dfrac{h}{\sqrt{2}l}\right)+1\right)}{3\sqrt{2}\sinh\left(\dfrac{h}{\sqrt{2}l}\right)-\dfrac{h}{l}}-\dfrac{2l}{h}\right\} & \text{for } \dfrac{4M^2l^2}{{h_{ms}}^2}=1\\ \dfrac{6{h_{ms}}^2h^2}{\mu lM^2}\left\{\dfrac{M\left(\cos\beta_1 h+\cosh\alpha_1 h\right)}{h_{ms}\left(\alpha_2\sin\beta_1 h+\beta_2\sinh\alpha_1 h\right)}-\dfrac{2l}{h}\right\} & \text{for } \dfrac{4M^2l^2}{{h_{ms}}^2}>1\end{cases} \tag{10}$$

$$\alpha=\left\{\left(1+\sqrt{1-(4l^2M^2/h_{ms}^2)}\right)\Big/2\right\}^{1/2},$$

$$\beta=\left\{\left(1-\sqrt{1-(4l^2M^2/h_{ms}^2)}\right)\Big/2\right\}^{1/2},$$

$$\alpha_2=\left(\beta_1-\alpha_1\cot\varphi\right),\ \beta_2=\left(\alpha_1+\beta_1\cot\varphi\right),$$

$$\alpha_1=\sqrt{M/lh_{ms}}\cos\left(\varphi/2\right),\quad \beta_1=\sqrt{M/lh_{ms}}\sin\left(\varphi/2\right),$$

$$\varphi=\tan^{-1}\left(\sqrt{(4l^2M^2/{h_{ms}}^2)-1}\right)$$

The modified Reynolds type equation (9) is applicable to one-dimensional slider bearings lubricated with couple stress fluid in the presence of transverse magnetic field with the squeezing effect $\partial h/\partial t$. The thickness of fluid film in the flow region is given by $h=h(x,t)$. In the present study, the exponential slider bearing is considered and its geometrical configuration is shown in Fig. 1. The mathematical function for the film thickness is given by:

$$h(x,t)=h_m(t)\cdot\exp\left\{-\frac{x}{L}\ln\left(\frac{h_1(t)}{h_m(t)}\right)\right\} \tag{11}$$

where $h_m(t)$ is the minimum film thickness, $h_1(t)=d+h_m(t)$ is the inlet film thickness and d is the difference between inlet and outlet film thicknesses.

Defining the non-dimensional quantities, $\bar{x}=\frac{x}{L}$, $\bar{p}=\frac{ph_{ms}^2}{\mu UL}$, $\bar{h}_m=\frac{h_m(t)}{h_{ms}}$, $\bar{h}=\frac{h}{h_{ms}}$, $\bar{t}=\frac{Ut}{L}$, $\bar{l}=\frac{2l}{h_{ms}}$ and using these in equation (9), the non-dimensional Reynolds type equation is obtained as:

$$\frac{\partial}{\partial\bar{x}}\left[\bar{G}\left(\bar{h},\bar{l},M\right)\frac{\partial\bar{p}}{\partial\bar{x}}\right]=6\frac{\partial\bar{h}}{\partial\bar{x}}+12\frac{\partial\bar{h}}{\partial\bar{t}} \tag{12}$$

where,

$\bar{G}\left(\bar{h},\bar{l},M\right)$

$$=\begin{cases}\dfrac{12\bar{h}^2}{\bar{l}M^2}\left\{\dfrac{\bar{\alpha}^2-\bar{\beta}^2}{\dfrac{\bar{\alpha}^2}{\bar{\beta}}\tanh\left(\dfrac{\bar{\beta}\bar{h}}{\bar{l}}\right)-\dfrac{\bar{\beta}^2}{\bar{\alpha}}\tanh\left(\dfrac{\bar{\alpha}\bar{h}}{\bar{l}}\right)}-\dfrac{\bar{l}}{\bar{h}}\right\} & \text{for } M^2\bar{l}^2<1\\ \dfrac{12\bar{h}^2}{\bar{l}M^2}\left\{\dfrac{1+\cosh\left(\dfrac{\sqrt{2}\bar{h}}{\bar{l}}\right)}{\dfrac{3}{\sqrt{2}}\sinh\left(\dfrac{\sqrt{2}\bar{h}}{\bar{l}}\right)-\dfrac{\bar{h}}{\bar{l}}}-\dfrac{\bar{l}}{\bar{h}}\right\} & \text{for } M^2\bar{l}^2=1\\ \dfrac{12\bar{h}^2}{\bar{l}M^2}\left\{\dfrac{M\left(\cos\bar{\beta}_1\bar{h}+\cosh\bar{\alpha}_1\bar{h}\right)}{\bar{\alpha}_2\sin\bar{\beta}_1\bar{h}+\bar{\beta}_2\sinh\bar{\alpha}_1\bar{h}}-\dfrac{\bar{l}}{\bar{h}}\right\} & \text{for } M^2\bar{l}^2>1\end{cases} \tag{13}$$

$$\bar{\alpha}=\left\{\left(1+\left(1-\bar{l}M^2\right)^{1/2}\right)\Big/2\right\}^{1/2},$$

$$\bar{\beta}=\left\{\left(1-\left(1-\bar{l}M^2\right)^{1/2}\right)\Big/2\right\}^{1/2},$$

$$\bar{\alpha}_1=\sqrt{2M/\bar{l}}\cos\left(\bar{\varphi}/2\right),\quad \bar{\beta}_1=\sqrt{2M/\bar{l}}\sin\left(\bar{\varphi}/2\right),$$

$$\bar{\alpha}_2=\left(\bar{\beta}_1-\bar{\alpha}_1\cot\bar{\varphi}\right),\quad \bar{\beta}_2=\left(\bar{\alpha}_1+\bar{\beta}_1\cot\bar{\varphi}\right)$$

$$\bar{\varphi}=\tan^{-1}\left(\sqrt{\bar{l}M^2-1}\right)$$

$$\bar{h}(\bar{x},\bar{t})=\frac{h(x,t)}{h_{ms}} \tag{14}$$

$$\bar{h}(\bar{x},\bar{t})=\bar{h}_m(\bar{t})\cdot\exp\left\{-\bar{x}\ln\left(\delta+1\right)\right\} \tag{15}$$

and $\delta\left(=\dfrac{d}{h_{ms}}\right)$ being the profile parameter.

The pressure boundary conditions are given by:

$$\bar{p}=0 \text{ at } \bar{x}=0 \text{ and } \bar{x}=-1 \tag{16}$$

With the use of pressure boundary conditions, the twice integration of the non-dimensional Reynolds type equation (12) with respect to $\bar{x}$ gives the expression for film pressure in the form:

$$\bar{p}=\left[6\bar{h}_m(\bar{t})-\frac{12}{\ln\left(\delta+1\right)}\bar{V}\right]\xi_A\left(\bar{x},\bar{h}_m\right)+\chi_1\left(\bar{h}_m,\bar{V}\right)\xi_B\left(\bar{x},\bar{h}_m\right) \tag{17}$$

where $\bar{V}=d\bar{h}_m/d\bar{t}$ represents squeezing velocity in the non-dimensional form:

$$\xi_A\left(\bar{x},\bar{h}_m\right)=\int_{\bar{x}=0}^{\bar{x}}\frac{\exp\left\{-\bar{x}\ln\left(\delta+1\right)\right\}}{\bar{G}(\bar{h},\bar{l},M)}d\bar{x} \tag{18}$$

$$\xi_B\left(\bar{x},\bar{h}_m\right)=\int_{\bar{x}=0}^{\bar{x}}\frac{1}{\bar{G}(\bar{h},\bar{l},M)}d\bar{x} \tag{19}$$

$$\chi_1\left(\bar{h}_m,\bar{V}\right)=-\left[6\bar{h}_m(\bar{t})-\frac{12}{\ln\left(\delta+1\right)}\bar{V}\right]\left[\frac{\xi_{AM1}\left(\bar{h}_m\right)}{\xi_{BM1}\left(\bar{h}_m\right)}\right] \tag{20}$$

where $\xi_{AM1}(\bar{h}_m)$ and $\xi_{BM1}(\bar{h}_m)$ are given as follows:

$$\xi_{AM1}\left(\bar{h}_m\right)=\int_{\bar{x}=0}^{-1}\frac{\exp\left\{-\bar{x}\ln\left(\delta+1\right)\right\}}{\bar{G}(\bar{h},\bar{l},M)}d\bar{x} \tag{21}$$

$$\xi_{BM1}\left(\bar{h}_m\right)=\int_{\bar{x}=0}^{-1}\frac{1}{\bar{G}(\bar{h},\bar{l},M)}d\bar{x} \tag{22}$$

By integrating the non-dimensional film pressure over the film region non-dimensional film force is obtained in the form:

$$\bar{F}=\frac{Fh_{ms}{}^2}{\mu UL^2B_0}=-\int_{\bar{x}=0}^{-1}\bar{p}\,d\bar{x} \tag{23}$$

where F is the film force and substituting the value of non-dimensional pressure expression from equation (17) in equation (23), the expression for $\bar{F}$ is obtained as:

$$\bar{F}=-\left\{6\bar{h}_m(\bar{t})-\frac{12}{\ln\left(\delta+1\right)}\bar{V}\right\}g_A\left(\bar{h}_m\right)-\chi_1\left(\bar{h}_m,\bar{V}\right)g_B\left(\bar{h}_m\right) \tag{24}$$

where g_A and g_B are determined by the following double integrals:

$$g_A(\bar{h}_m)=\int_{\bar{x}=0}^{-1}\int_{\bar{x}=0}^{\bar{x}}\frac{\exp\left\{-\bar{x}\ln\left(\delta+1\right)\right\}}{\bar{G}(\bar{h},\bar{l},M)}d\bar{x}d\bar{x} \tag{25}$$

$$g_B(\bar{h}_m)=\int_{\bar{x}=0}^{-1}\int_{\bar{x}=0}^{\bar{x}}\frac{1}{\bar{G}(\bar{h},\bar{l},M)}d\bar{x}d\bar{x} \tag{26}$$

3.1 Steady state characteristics

Let the non-dimensional minimum film height be constant and the non-dimensional squeezing velocity be zero. From equations (17) and (24), the expressions for the steady film pressure and the steady load carrying capacity in non-dimensional for are obtained as:

$$\bar{p}_s=6\left(\bar{h}_m\right)_s\left[\xi_A\left(\bar{x},\bar{h}_m\right)\right]_s+\left[\chi_1\right]_s\left[\xi_B\left(\bar{x},\bar{h}_m\right)\right]_s \tag{27}$$

$$\bar{W}_s=-6\left[\bar{h}_m\right]_s\left[g_A\left(\bar{h}_m\right)\right]_s-\left[\chi_1\right]_s\left[g_B\left(\bar{h}_m\right)\right]_s \tag{28}$$

3.2 Dynamic characteristics

The partial derivative of film force in non-dimensional form with respect to minimum film thickness in non-dimensional form under steady state gives dynamic stiffness coefficient in non-dimensional form as:

$$\bar{S}_d=-\left(\frac{\partial\bar{F}}{\partial\bar{h}_m}\right)_s=6\left(\bar{h}_m\right)_s\left(\frac{\partial g_A}{\partial\bar{h}_m}\right)_s+6\left(g_A\left(\bar{h}_m\right)\right)_s+\left(\chi_1\right)_s\left(\frac{\partial g_B}{\partial\bar{h}_m}\right)_s+\left(g_B\left(\bar{h}_m\right)\right)_s\left(\frac{\partial\chi_1}{\partial\bar{h}_m}\right)_s \tag{29}$$

where subscript s denotes the steady state.

$$\frac{\partial g_A}{\partial\bar{h}_m}=-\int_{\bar{x}=0}^{-1}\int_{\bar{x}=0}^{\bar{x}}\frac{\exp\left\{-\bar{x}\ln\left(\delta+1\right)\right\}}{\left\{\bar{G}(\bar{h},\bar{l},M)\right\}^2}\frac{\partial\bar{G}}{\partial\bar{h}_m}d\bar{x}d\bar{x} \tag{30}$$

$$\frac{\partial g_B}{\partial \bar{h}} = -\int_{\bar{x}=0}^{-1}\int_{\bar{x}=0}^{\bar{x}} \frac{1}{\left\{\bar{G}(\bar{h},\bar{l},M)\right\}^2}\frac{\partial \bar{G}}{\partial \bar{h}_m}\,d\bar{x}d\bar{x} \tag{31}$$

$$\left(\frac{\partial \chi_1}{\partial \bar{h}_m}\right)_s = \frac{-6}{\left\{\xi_{BM1}\right\}_s^2}\left[\begin{array}{c}\xi_{CM1}\left\{\xi_{AM1}+\bar{h}_m\dfrac{\partial \xi_{AM1}}{\partial \bar{h}_m}\right\}\\ -\bar{h}_m\xi_{AM1}\dfrac{\partial \xi_{BM1}}{\partial \bar{h}_m}\end{array}\right]_s \tag{32}$$

$$\frac{\partial \xi_{AM1}}{\partial \bar{h}_m} = -\int_{\bar{x}=0}^{-1}\frac{\exp\left\{-\bar{x}\ln(\delta+1)\right\}}{\left\{\bar{G}(\bar{h},\bar{l},M)\right\}^2}\frac{\partial \bar{G}}{\partial \bar{h}_m}\,d\bar{x} \tag{33}$$

$$\frac{\partial \xi_{BM1}}{\partial \bar{h}_m} = -\int_{\bar{x}=0}^{-1}\frac{1}{\left\{\bar{G}(\bar{h},\bar{l},M)\right\}^2}\frac{\partial \bar{G}}{\partial \bar{h}_m}\,d\bar{x} \tag{34}$$

The partial derivative of film force in non-dimensional form with respect to squeezing velocity in non-dimensional form under steady state gives the dynamic damping coefficient in non-dimensional form as:

$$\bar{C}_d = -\left(\frac{\partial \bar{F}}{\partial \bar{V}}\right)_s = -\frac{12}{\ln(\delta+1)}\left[g_A - \frac{\xi_{AM1}}{\xi_{BM1}}g_B\right]_s \tag{35}$$

4. RESULTS AND DISCUSSION

The numerical integration of integrals appearing in the expressions for film force, dynamic stiffness and damping coefficients are performed by using the quadrature formula. The Hartmann number M characterizes the effect of externally applied magnetic field and the parameter $\bar{l}$ characterizes the effect of couple stresses. The static and dynamic characteristics of exponential slider bearing lubricated with couple stress fluid in the presence of applied transverse magnetic field is analyzed in the present paper. The results of Lin and Lu [20] can be recovered in the limiting case as $\bar{l} \to 0$ for the conducting Newtonian case. While $M \to 0$ the results of Lin and Hung [19] can be recovered from the present analysis. The flow chart for the computation of $\bar{p}_s$, $\bar{W}_s$, $\bar{S}_d$ and $\bar{C}_d$ is shown in Fig. 2.

4.1 Steady film pressure

The variation of non-dimensional film pressure $\bar{p}_s$ with the non-dimensional coordinate $\bar{x}$ for different values of Hartmann number M and couple stress parameter $\bar{l}$ with $\delta = 1, \bar{h}_{ms} = 1$ and $\bar{l} = 0.4$ is shown in Fig. 3. Compared to Newtonian case ($\bar{l} = 0$), the effect of couple stress is to increase the values of $\bar{p}_s$ with $\bar{x}$. It is observed that the application of magnetic field increases the steady state pressure even bearings are lubricated with couple stress fluid compared to non-magnetic case. The reason for the increase in the pressure is the retention of large amount of lubricant in the film region due to reduced velocity of lubricant on the application the magnetic field.

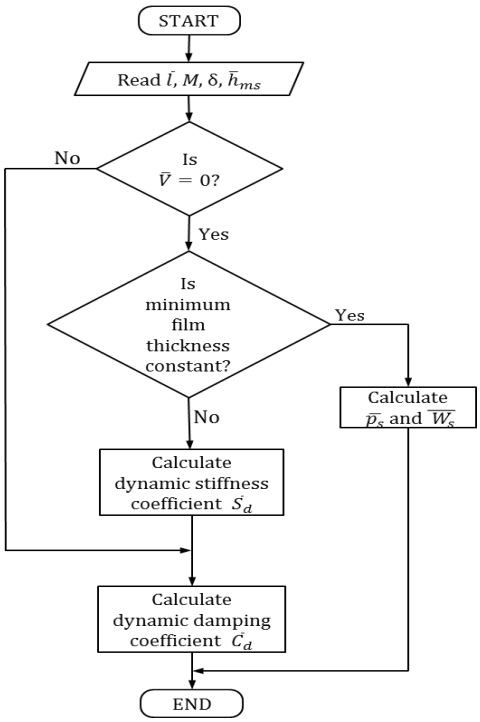

Fig. 2. Flow chart of computation.

Figure 4 depicts the variation of non-dimensional steady maximum film pressure $\bar{p}_{sm}$ with profile parameter δ for different values of M and $\bar{l}$ under $\bar{h}_{ms} = 1$. It is found that the effect of couple stresses is to increase the values of $\bar{p}_{sm}$ as compared to Newtonian case. The applied magnetic field also increases the value of $\bar{p}_{sm}$ even bearing is lubricated with couple stress fluid. The variation of $\bar{p}_{sm}$ with non-dimensional steady minimum film thickness $\bar{h}_{ms}$ for different values M and $\bar{l}$ under $\delta = 1$ is shown in Fig. 5. It is observed that the value of $\bar{p}_{sm}$ increases for the couple stress fluid as compared to Newtonian case. The value of $\bar{p}_{sm}$ increases with decrease in the value of $\bar{h}_{ms}$ which implies that the maximum pressure is generated in the film region for lower film thickness.

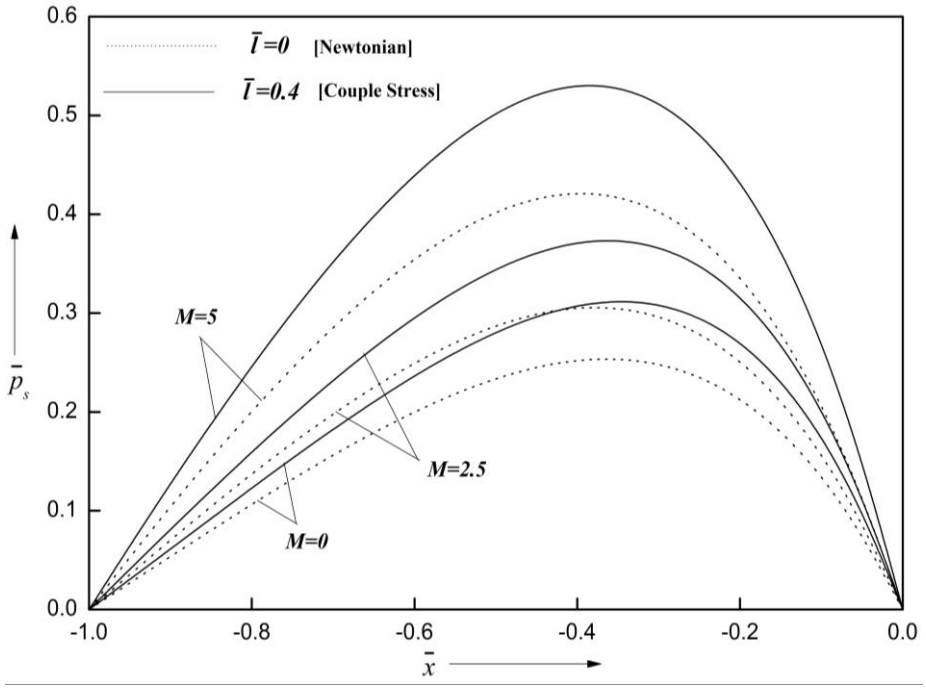

Fig. 3. Non-dimensional steady film pressure $\bar{p}_s$ with $\bar{x}$ for different values of M and $\bar{l}$ with $\delta=1$, $\bar{h}_{ms}=1$.

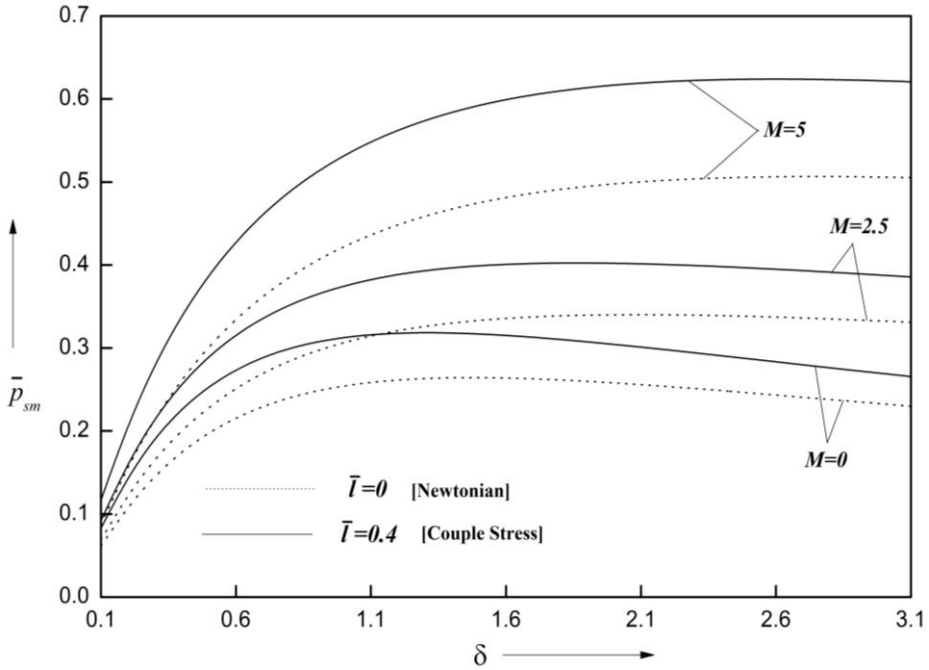

Fig. 4. Non-dimensional steady maximum film pressure $\bar{p}_{sm}$ with δ for different values of M and $\bar{l}$ with $\bar{h}_{ms}=1$.

4.2 Steady load carrying capacity

The variation of non-dimensional steady load carrying capacity $\bar{W}_s$ with profile parameter δ for different values of M and $\bar{l}$ under $\bar{h}_{ms}=1$ is shown in Fig. 6. Both the application of magnetic field and effect of couple stresses increase the value of $\bar{W}_s$ as compared to non-magnetic and Newtonian case. The value of $\bar{W}_s$ increases with increases in the value of δ till it attains maximum and thereafter it decreases. It is observed that in both Newtonian and non-magnetic cases the steady load carrying capacity decreases for higher value of δ but this trend changes with presence application of external magnetic field.

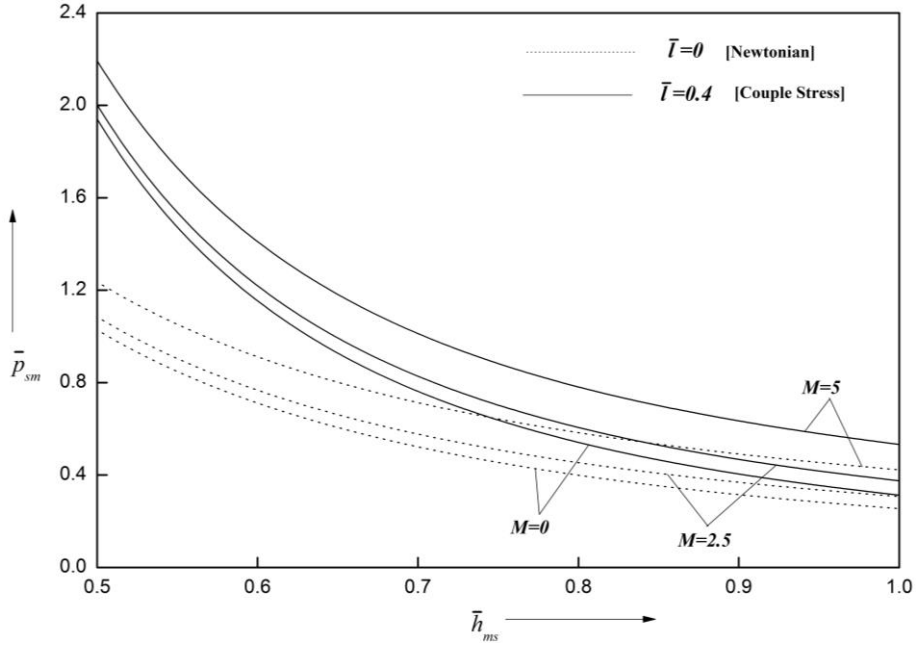

Fig. 5. Non-dimensional steady maximum film pressure $\bar{p}_{sm}$ with $\bar{h}_{ms}$ for different values of M and $\bar{l}$ with $\delta=1$.

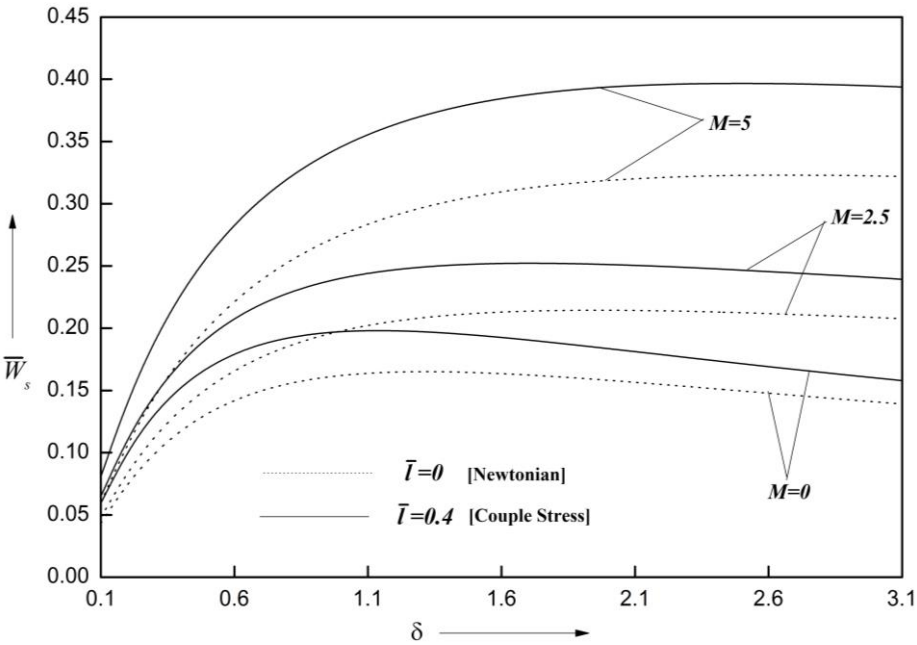

Fig. 6. Non-dimensional steady load carrying capacity $\bar{W}_s$ with δ for different values of M and $\bar{l}$ with $\bar{h}_{ms}=1$.

The variation of $\bar{W}_s$ with non-dimensional steady minimum film thickness $\bar{h}_{ms}$ for different values M and $\bar{l}$ under $\delta=1$ is shown in Fig. 7. The presence of couple stresses and external applied magnetic field enhances the steady load carrying capacity irrespective of film thickness. The load carrying capacity increases due to the increase in pressure as the result of reduced velocity of lubricant on the application magnetic field. With the decrease in the value of $\bar{h}_{ms}$, the increase in the value of $\bar{W}_s$ is observed and for lower film thickness maximum value of $\bar{W}_s$ is obtained.

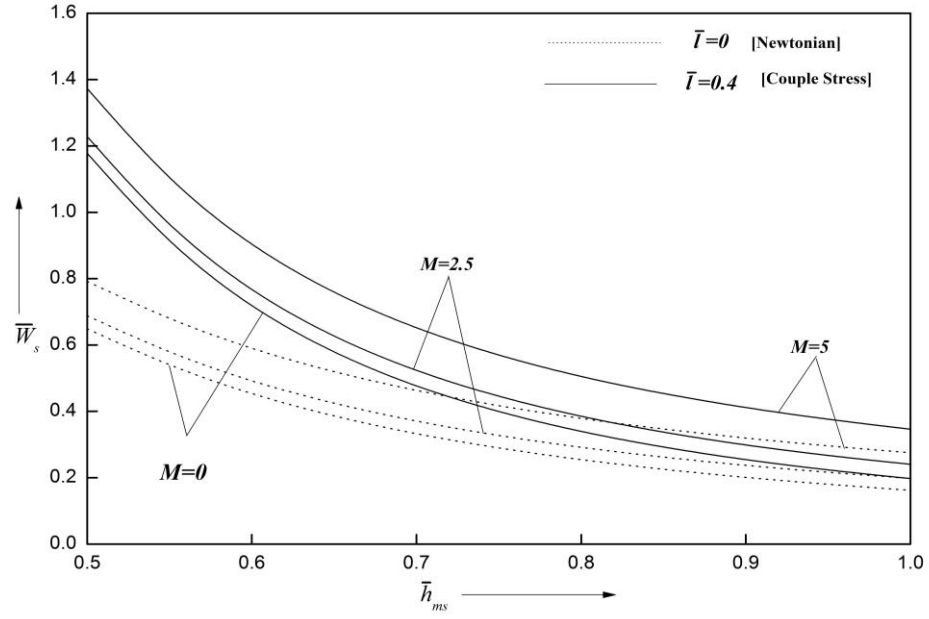

Fig. 7. Non-dimensional steady load carrying capacity $\bar{W}_s$ with $\bar{h}_{ms}$ for different values of M and $\bar{l}$ with $\delta=1$.

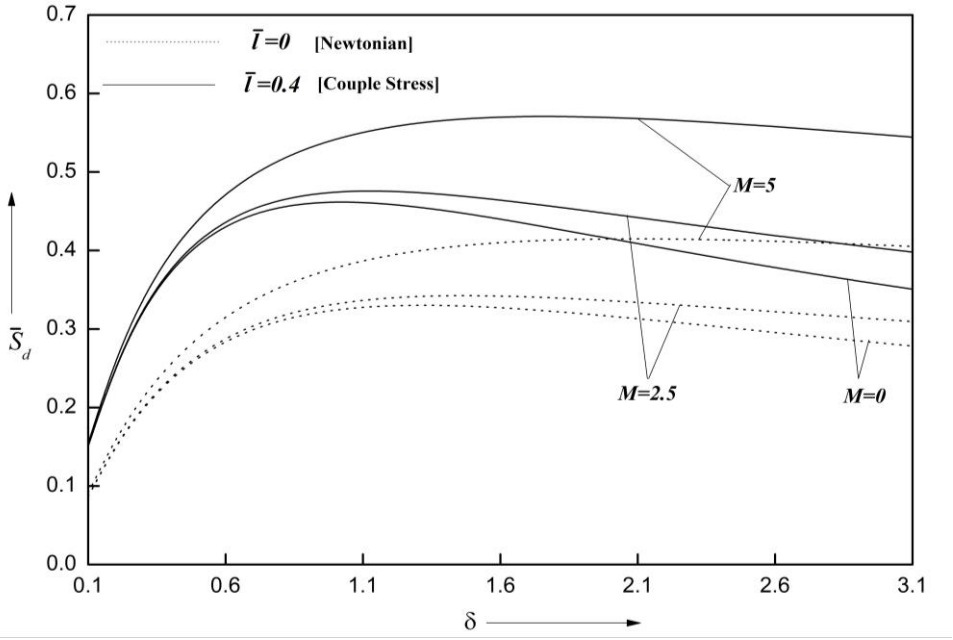

Fig. 8. Non-dimensional dynamic stiffness coefficient $\bar{S}_d$ with δ for different values of M and $\bar{l}$ with $\bar{h}_{ms}=1$.

4.3 Dynamic stiffness coefficient

The variation of non-dimensional dynamic stiffness coefficient $\bar{S}_d$ with profile parameter δ for different values M and $\bar{l}$ under $\bar{h}_{ms}=1$ is shown in Fig. 8. The value of $\bar{S}_d$ is to increase with increase in the values of $\bar{l}$ and M as compared to Newtonian and non-magnetic cases. The value of $\bar{S}_d$ increases with increase in δ until it attain maximum and thereafter it decreases. The variation of $\bar{S}_d$ with non-dimensional steady minimum film thickness $\bar{h}_{ms}$ for different values M and $\bar{l}$ under $\delta=1$ is shown in Fig. 9. The application of magnetic field and effect of couple stresses both increases the value of $\bar{S}_d$ as compared non-magnetic case and Newtonian cases. The value of $\bar{S}_d$ increases with decrease in the value of $\bar{h}_{ms}$ and the maximum value of $\bar{S}_d$ is obtained at lower value of film thickness. It is found that the effect of magnetic field is less compared to effect of couple stress in increasing the value of $\bar{S}_d$.

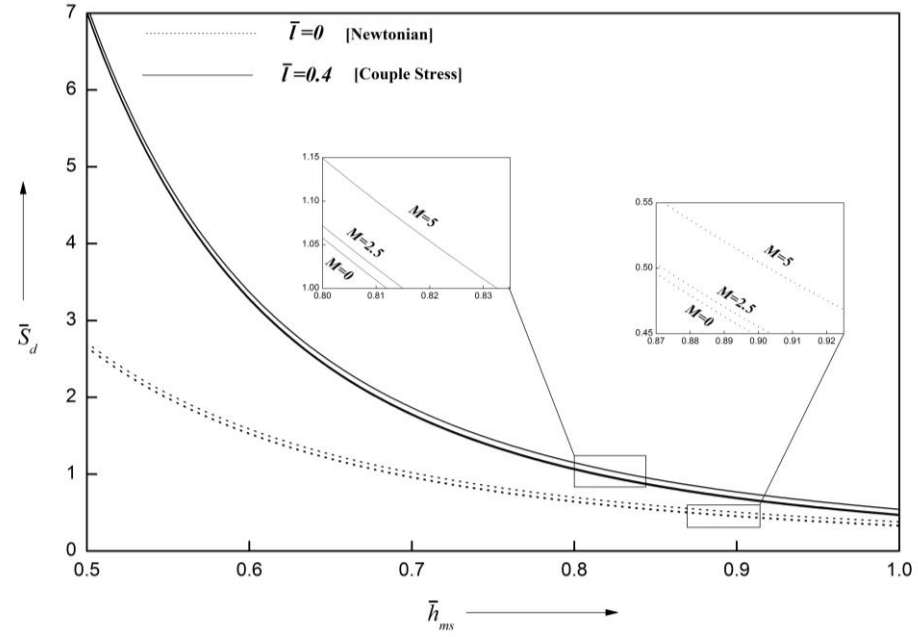

Fig. 9. Non-dimensional dynamic stiffness coefficient $\bar{S}_d$ with $\bar{h}_{ms}$ for different values of M and $\bar{l}$ with $\delta=1$.

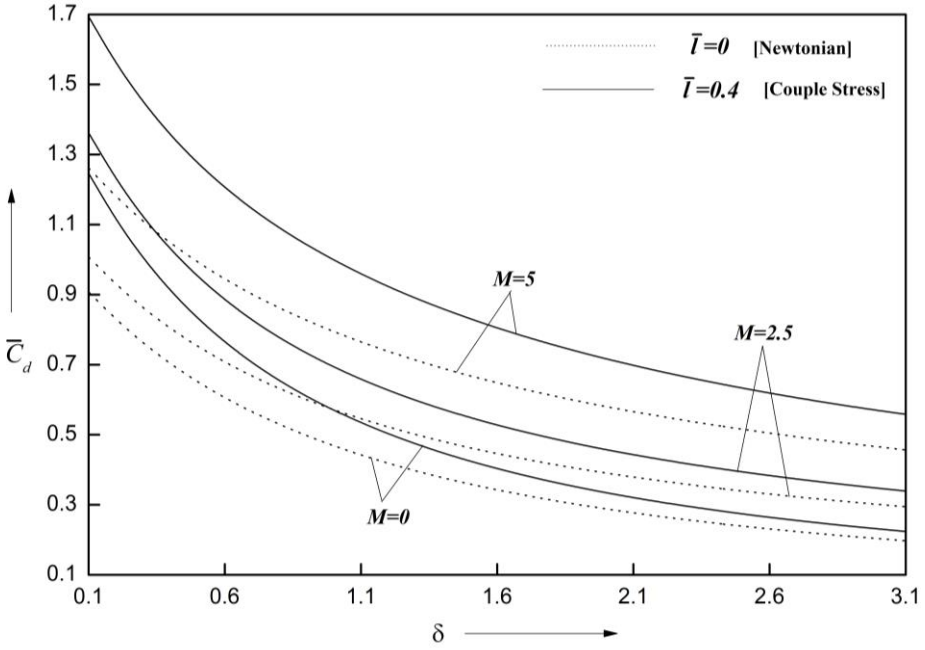

Fig. 10. Non-dimensional dynamic damping coefficient $\bar{C}_d$ with δ for different values of M and $\bar{l}$ with $\bar{h}_{ms}=1$.

4.4 Dynamic damping coefficient

The variation of non-dimensional dynamic damping coefficient $\bar{C}_d$ with profile parameter δ for different values M and $\bar{l}$ under $\bar{h}_{ms}=1$ is shown in Figure 10. It is found that the value of $\bar{C}_d$ increases with increases in the value of $\bar{l}$ and M as compared to Newtonian and non-magnetic case. The value of $\bar{C}_d$ increases with decrease in the value of δ. The variation of $\bar{C}_d$ with non-dimensional $\bar{h}_{ms}$ for different values of M and $\bar{l}$ under $\delta=1$ is shown in Fig. 11. It is observed that the increase in values of $\bar{l}$ and M increases the value of $\bar{C}_d$ compared to Newtonian and non-magnetic cases.

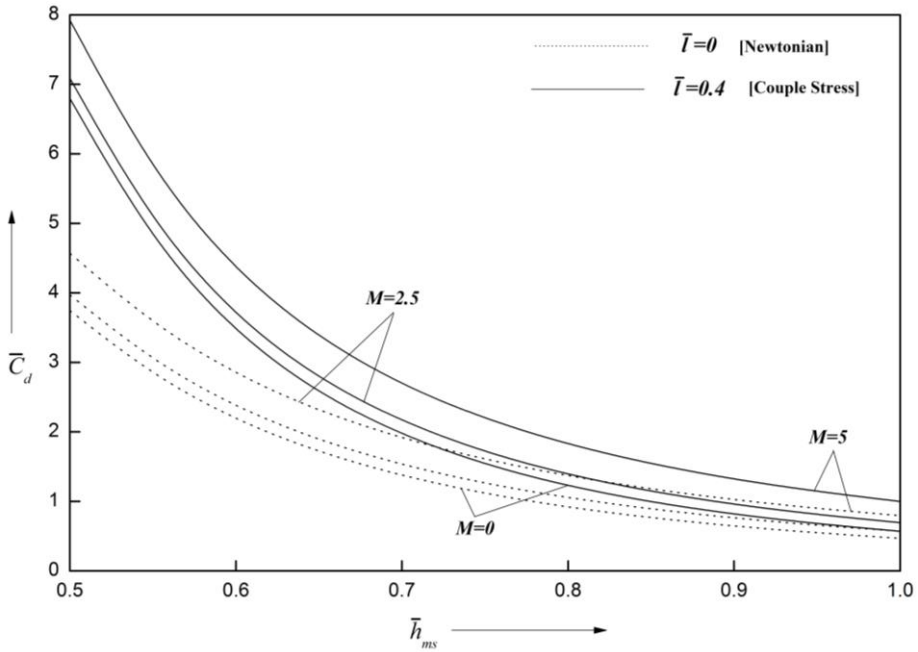

Fig. 11. Non-dimensional dynamic damping coefficient $\bar{C}_d$ with $\bar{h}_{ms}$ for different values of M and $\bar{l}$ with $\delta = 1$.

Table 1. Design example of slider bearing lubricated with couple stress fluid in presence of magnetic field considering squeezing effect irrespective of the bearing shape.

Physical quantity	Symbol	Value of Physical quantity
Length of the bearing	L	$1.0\times10^{-1}\,m$
Inlet film thickness	h_1	$(1.5, 2.0, 2.5, 3.0, 3.5)\times10^{-4}\,m$
Outlet film thickness	$\bar{h}_{ms}$	$1.0\times10^{-4}\,m$
Profile parameter	δ	$0.5, 1.0, 1.5, 2.0, 2.5$
Electrical conductivity	σ	$1.07\times10^{6}\,mho/m$
Lubricant viscosity	μ	$1.55\times10^{-3}\,Pa.s$
Applied magnetic field	B_0	$0, 0.95, 1.90\,Wb/m^2$
Couple stress material constant	η	$(0, 0.3875, 1.55, 3.4875, 6.2)\times10^{-13}\,Ns$

4.5 Design example

A design example for exponential slider bearing lubricated with couple stress fluid in presence of transverse magnetic field is presented for the use of this work in the bearing design by engineers with the physical quantities whose values are given in Table 1. For these considered physical quantities the values of couple stress parameter and Hartmann number are obtained as $\bar{l} = 0, 0.1, 0.2, 0.3, 0.4$ and $M = 0, 2.5, 5$ respectively. These numerical values are so chosen to cover all the three cases in the equation (13). Further, the values of steady load carrying capacity, dynamic stiffness coefficient and dynamic damping coefficient are obtained using the expressions obtained in the previous section with considered values of physical quantities and are given in Tables 2, 3 and 4 respectively. These values are useful for engineers in the designing of bearings.

5. CONCLUSION

The modified Reynolds type equation is obtained to study the effect of couple stresses on static and dynamic characteristics of exponential slider bearing in the presence of magnetic field. The effects of couple stresses and the applied transverse magnetic field is to increase the steady film pressure, the steady load carrying capacity, the dynamic stiffness coefficient and dynamic damping coefficient as

compared to the corresponding Newtonian case and the non-magnetic case respectively. Hence the exponential slider bearing lubricated with the couple stress fluid in the presence of applied magnetic field provides improved efficiency with larger couple stress parameter and Hartmann number for smaller values of profile parameter.

Table 2. Values for non-dimensional steady state load carrying capacity $\bar{W}_s$ with $\bar{h}_{ms}=1$.

M	δ	Lin and Hung[19]	Lin and Lu[20]	Present Analysis				
		$\bar{l}=0$	$\bar{l}=0$	$\bar{l}=0$	$\bar{l}=0.1$	$\bar{l}=0.2$	$\bar{l}=0.3$	$\bar{l}=0.4$
0	0.5	0.13	0.1320	0.1320	0.1345	0.1416	0.1530	0.1687
	1.0	0.16	0.1622	0.1622	0.1647	0.1715	0.1825	0.1974
	1.5	0.16	0.1644	0.1644	0.1665	0.1724	0.1818	0.1944
	2.0	0.15	0.1582	0.1582	0.1600	0.1650	0.1730	0.1836
	2.5	0.14	0.1496	0.1496	0.1512	0.1555	0.1626	0.1715
	3.0	0.14	0.1409	0.1409	0.1422	0.1460	0.1520	0.1601
2.5	0.5	-	0.1525	0.1525	0.1557	0.1640	0.1764	0.1929
	1.0	-	0.1980	0.1980	0.2015	0.2104	0.2234	0.2403
	1.5	-	0.2119	0.2119	0.2153	0.2237	0.2360	0.2515
	2.0	-	0.2144	0.2144	0.2176	0.2255	0.2369	0.2511
	2.5	-	0.2124	0.2124	0.2154	0.2228	0.2334	0.2466
	3.0	-	0.2085	0.2085	0.2114	0.2184	0.2283	0.2406
5	0.5	-	0.2012	0.2012	0.2077	0.2221	0.2383	0.2585
	1.0	-	0.2752	0.2752	0.2836	0.3006	0.3218	0.3461
	1.5	-	0.3061	0.3061	0.3151	0.3331	0.3554	0.3807
	2.0	-	0.3188	0.3188	0.3279	0.34611	0.3685	0.3937
	2.5	-	0.3228	0.3228	0.3318	0.3498	0.3719	0.3966
	3.0	-	0.3224	0.3223	0.3312	0.3488	0.3704	0.3946

Table 3. Values for non-dimensional dynamic stiffness coefficient $\bar{S}_d$ with $\bar{h}_{ms}=1$.

M	δ	Lin and Hung[19]	Lin and Lu[20]	Present Analysis				
		$\bar{l}=0$	$\bar{l}=0$	$\bar{l}=0$	$\bar{l}=0.1$	$\bar{l}=0.2$	$\bar{l}=0.3$	$\bar{l}=0.4$
0	0.5	0.26	0.2639	0.2639	0.2738	0.3017	0.3467	0.4085
	1.0	0.32	0.3244	0.3244	0.3340	0.3610	0.4038	0.4620
	1.5	0.33	0.3289	0.3289	0.3372	0.3602	0.3967	0.4457
	2.0	0.32	0.3164	0.3163	0.3234	0.3431	0.3740	0.4152
	2.5	0.30	0.2992	0.2992	0.3053	0.3223	0.3489	0.3841
	3.0	0.28	0.2817	0.2817	0.2871	0.3020	0.3252	0.3560
2.5	0.5	-	0.2668	0.2668	0.2776	0.3061	0.3512	0.4128
	1.0	-	0.3321	0.3321	0.3431	0.3718	0.4158	0.4747
	1.5	-	0.3425	0.3425	0.3524	0.3782	0.4171	0.4680
	2.0	-	0.3360	0.3360	0.3450	0.3680	0.4023	0.4467
	2.5	-	0.3245	0.3245	0.3326	0.3534	0.3842	0.4235
	3.0	-	0.3120	0.3120	0.3194	0.3384	0.3664	0.4019
5	0.5	-	0.2894	0.2895	0.3036	0.3350	0.3800	0.4402
	1.0	-	0.3781	0.3781	0.3944	0.4301	0.4794	0.5419
	1.5	-	0.4073	0.4073	0.4238	0.4595	0.5080	0.5683
	2.0	-	0.4146	0.4146	0.4307	0.4652	0.5118	0.5693
	2.5	-	0.4127	0.4127	0.4281	0.4612	0.5056	0.5602
	3.0	-	0.4066	0.4066	0.4214	0.4531	0.4954	0.5472

Table 4. Values for non-dimensional dynamic damping coefficient $\bar{C}_d$ with $\bar{h}_{ms}=1$.

M	δ	Lin and Hung[19]	Lin and Lu[20]	Present Analysis				
		$\bar{l}=0$	$\bar{l}=0$	$\bar{l}=0$	$\bar{l}=0.1$	$\bar{l}=0.2$	$\bar{l}=0.3$	$\bar{l}=0.4$
0	0.5	0.65	0.6509	0.6509	0.6633	0.6984	0.7548	0.8321
	1.0	0.47	0.4681	0.4680	0.4751	0.4949	0.5266	0.5695
	1.5	0.36	0.3589	0.3589	0.3635	0.3764	0.3968	0.4244
	2.0	0.29	0.2880	0.2879	0.2912	0.3004	0.3149	0.3343
	2.5	0.24	0.2389	0.2388	0.2413	0.2483	0.2592	0.2738
	3.0	0.20	0.2032	0.2032	0.2052	0.2107	0.2194	0.2309
2.5	0.5	-	0.7520	0.7520	0.7680	0.8088	0.8703	0.9516
	1.0	-	0.5712	0.5712	0.5814	0.6071	0.6447	0.6932
	1.5	-	0.4625	0.4625	0.4699	0.4883	0.5150	0.5489
	2.0	-	0.3903	0.3903	0.3962	0.4106	0.4312	0.4572
	2.5	-	0.3391	0.3391	0.3439	0.3558	0.3726	0.3937
	3.0	-	0.3008	0.3008	0.3050	0.3150	0.3293	0.3471
5	0.5	-	0.9925	0.9924	1.0247	1.0912	1.1756	1.2754
	1.0	-	0.7942	0.7942	0.8183	0.8674	0.9284	0.9986
	1.5	-	0.6682	0.6682	0.6877	0.7271	0.7758	0.8310
	2.0	-	0.5804	0.5804	0.5969	0.6300	0.6708	0.7168
	2.5	-	0.5154	0.5153	0.5297	0.5585	0.5937	0.6332
	3.0	-	0.4650	0.4650	0.4778	0.5033	0.5344	0.5692

Nomenclature

B_0 applied magnetic field

$\bar{C}_d$ non-dimensional dynamic damping coefficient

d difference between the inlet and outlet film thickness

E_z induced electric field in the z - direction

F, $\bar{F}$ film force, $\bar{F}=\dfrac{Fh_{ms}^2}{\mu UL^2B_0}$

$h(x,t)$ film thickness

$\bar{h}$ non-dimensional film thickness, $\bar{h}(\bar{x},\bar{t})=h(x,t)/h_{ms}$

$h_m(t)$ minimum squeezing film thickness

$\bar{h}_m(\bar{t})$ non-dimensional minimum squeezing film thickness $\bar{h}_m(\bar{t})=h_m(t)/h_{ms}$

h_{ms} steady state reference minimum film thickness at outlet

h_1 inlet film thickness

L length of the bearing

l couple stress parameter

$\bar{l}$ non-dimensional couple stress parameter, $\bar{l}=2l/h_{ms}$

M Hartmann number, $M=B_0h_{ms}\left(\sigma/\mu\right)^{1/2}$

p film pressure

p_s steady film pressure

$\bar{p}$ non-dimensional film pressure, $\bar{p}=ph_{ms}^2/\mu UL$

$\bar{p}_s$ non-dimensional steady film pressure, $\bar{p}_s=p_sh_{ms}^2/\mu UL$

$\bar{p}_{sm}$ non-dimensional steady maximum film pressure

$\bar{S}_d$ non-dimensional dynamic damping coefficient

$t,\bar{t}$ time, $\bar{t}=Ut/L$

U sliding velocity of lower part

$\bar{V}$ non-dimensional squeezing velocity, $\bar{V}=d\bar{h}_m/d\bar{t}$

u, v velocity components in x and y directions

W_s steady load carrying capacity

$\bar{W}_s$ non-dimensional steady load carrying capacity,

x, y Cartesian coordinates

$\bar{x}$ non-dimensional coordinate $\bar{x} = x / L$

δ profile parameter $\delta = d / h_{ms}$

η material constant responsible for couple stress parameter

μ lubricant viscosity

σ conductivity of the lubricant

REFERENCES

[1] W.T. Snyder, 'The magnetohydrodynamic slider bearing', *Journal of Fluids Engineering*, vol. 84, no. 1, pp.197-202, 1962.

[2] W.F. Hughes, 'The magnetohydrodynamic inclined slider bearing with a transverse magnetic field', *Wear*, vol. 6, no. 4, pp. 315-324, 1963.

[3] W.F. Hughes, 'The magnetohydrodynamic finite step slider bearing', *Journal of Basic Engineering*, vol. 85, no. 1, pp. 129-136, 1963.

[4] D.C. Kuzma, 'The magnetohydrodynamic parallel plate slider bearing', *ASME Journal of Basic Enginnering*, vol. 87, no. 3, pp. 778-780, 1964.

[5] D.C. Kuzma, 'The magnetohydrodynamic journal bearing', *Journal of Basic Engineering*, vol. 85, no. 3, pp. 424-427, 1963.

[6] J.R. Lin, 'Magneto-hydrodynamic squeeze film characteristics for finite rectangular plates', *Industrial Lubrication and Tribology*, vol. 55, no. 2, pp. 84-89, 2003.

[7] V.K. Stokes, 'Couple stresses in fluids', *Physics of Fluids*, vol. 9, no. 9, pp. 1709-1715, 1966.

[8] G. Ramanaiah and P. Sarkar, 'Slider bearings lubricated by fluids with couple stress', *Wear*, vol. 52, no. 1, pp. 27-36, 1979.

[9] G.H. Ayyappa, N.B. Naduvinamani, A. Siddanagouda and S.N. Biradar, 'Effect of viscosity variation and surface roughness on the couple stress squeeze film characteristics of short journal bearing', *Tribology in Industry*, vol. 37, no. 1, pp. 117-127, 2015.

[10] N.B. Naduvinamani and A. Siddangouda, 'Squeeze film lubrication between circular stepped plates of couple stress fluids', *Journal of the Brazilian Society of Mechanical Sciences and Engineering*, vol. 31, no. 1, pp. 21-26, 2009.

[11] J.R. Lin, 'Squeeze film characteristic of long partial journal bearing lubricated with couple stress fluids', *Tribology International*, vol. 30, no. 1, pp. 53-58, 1997.

[12] A. Siddangouda, 'Squeezing film characteristics for micropolar fluid between porous parallel stepped plates', *Tribology in Industry*, vol. 37, no. 1, pp. 97-106, 2015.

[13] N.C. Das, 'A study of optimum load-bearing capacity for slider bearings lubricated with couple stress fluids in magnetic field', *Tribology International*, vol. 31, no. 7, pp. 393-400, 1998.

[14] N.B. Naduvinamani, S.T. Fathima and B.N. Hanumagowda, 'Magnetohydrodynamic couple stress squeeze film lubrication of circular stepped plates', *Proceedings of the Institution of Mechanical Engineers, Part J: Journal of Engineering Tribology*, vol. 225, no. 3, pp. 111-119, 2011.

[15] S.T. Fathima, N.B. Naduvinamani, B.N. Hanumagowda and J. Santoshkumar, 'Modified Reynolds Equation for Different Types of Finite Plates with the Combined Effect of MHD and Couple Stresses', *Tribology Transactions*, vol. 58, no. 4, pp. 660-667, 2015.

[16] J. Javorova, A. Mazdlakova, I. Andonov and A. Radulescu, 'Analysis of HD journal bearings considering elastic deformation and non-Newtonian Rabinowitsch fluid model', *Tribology in Industry*, vol. 38, no. 2, pp. 186-196, 2016.

[17] U.P. Singh, R.S. Gupta and V.K. Kapur, 'on the performance of pivoted curved slider bearings: Rabinowitsch fluid model', vol. 34, no. 3, pp. 128-137, 2012.

[18] J.R. Lin, C.R. Hung, C.H. Hsu and C. Lai, 'Dynamic stiffness and damping characteristics of one-dimensional magneto-hydrodynamic inclined-plane slider bearings', *Proceedings of the Institution of Mechanical Engineers, Part J: Journal of Engineering Tribology*, vol. 223, no. 2, pp. 211-219, 2009.

[19] J.R. Lin and C.R. Hung, 'Analysis of dynamic characteristics for wide slider bearings with an exponential film profile', *Journal of Marine Science and Technology*, vol. 12, no. 3, pp. 217-221, 2004.

[20] J.R. Lin and R.F. Lu, 'Dynamic characteristics for Magneto-hydrodynamic wide slider bearings with an exponential film profile', *Journal of Marine Science and Technology*, vol. 18, no. 2, pp. 268-276, 2010.

[21] N.B. Naduvinamani, A. Siddangouda and P. Siddharam, 'A comparative study of static and dynamic characteristics of parabolic and plane inclined slider bearings lubricated with MHD couple stress fluids', *Tribology Transactions,* vol. 60, no. 1, pp. 1-11, 2017.

Appendix A

$$\lambda_{11}=\frac{\beta^2}{\left(\alpha^2-\beta^2\right)}\left\{\frac{\sinh\left(\alpha h/l\right)-\sinh\left(\alpha y/l\right)+\sinh\left(\alpha\left(h-y\right)/l\right)}{\sinh\left(\alpha h/l\right)}\right\}$$

$$\lambda_{12}=\frac{\alpha^2}{\left(\alpha^2-\beta^2\right)}\left\{\frac{\sinh\left(\beta h/l\right)-\sinh\left(\beta y/l\right)+\sinh\left(\beta\left(h-y\right)/l\right)}{\sinh\left(\beta h/l\right)}\right\}$$

$$\lambda_{13}=\frac{\beta^2}{\frac{\beta^2}{\alpha}\tanh\left(\frac{\alpha h}{2l}\right)-\frac{\alpha^2}{\beta}\tanh\left(\frac{\beta h}{2l}\right)}\left\{\frac{\sinh\left(\frac{\alpha h}{l}\right)-\sinh\left(\frac{\alpha y}{l}\right)-\sinh\frac{\alpha\left(h-y\right)}{l}}{\sinh\left(\frac{\alpha h}{l}\right)}\right\}$$

$$\lambda_{14}=\frac{\alpha^2}{\frac{\beta^2}{\alpha}\tanh\left(\frac{\alpha h}{2l}\right)-\frac{\alpha^2}{\beta}\tanh\left(\frac{\beta h}{2l}\right)}\left\{\frac{\sinh\left(\frac{\beta h}{l}\right)-\sinh\left(\frac{\beta y}{l}\right)-\sinh\frac{\beta\left(h-y\right)}{l}}{\sinh\left(\frac{\beta h}{l}\right)}\right\}$$

$$\lambda_{21}=\frac{Sinh\left(\left(y-h\right)/\sqrt{2}l\right)+Sinh\left(y/\sqrt{2}l\right)-Sinh\left(h/\sqrt{2}l\right)}{Sinh\left(h/\sqrt{2}l\right)}$$

$$\lambda_{22}=\frac{yCosh\left(\left(y-h\right)/\sqrt{2}l\right)+yCosh\left(y/\sqrt{2}l\right)-h\,\mathrm{Coth}\left(h/2\sqrt{2}l\right)\mathrm{Sinh}\left(y/\sqrt{2}l\right)}{2\sqrt{2}l\,Sinh\left(h/\sqrt{2}l\right)}$$

$$\lambda_{23}=\frac{ySinh\left(\frac{y-h}{\sqrt{2}l}\right)+y\,\mathrm{Sinh}\left(\frac{y}{\sqrt{2}l}\right)-h\,\mathrm{Sinh}\left(\frac{y}{\sqrt{2}l}\right)}{\left(6l\,Sinh\left(\frac{h}{\sqrt{2}l}\right)-\sqrt{2}h\right)}$$

$$\lambda_{24}=\frac{2Cosh\left(\frac{y-h}{\sqrt{2}l}\right)+2Cosh\left(\frac{y}{\sqrt{2}l}\right)-2Cosh\left(\frac{h}{\sqrt{2}l}\right)-2}{\left(3\sqrt{2}Sinh\left(\frac{h}{\sqrt{2}l}\right)-\frac{h}{l}\right)}$$

$$\lambda_{31}=\frac{\mathrm{Cosh}\,\alpha_1 yCos\beta_1\left(y-h\right)-\mathrm{Cos}\,\beta_1 yCosh\alpha_1\left(y-h\right)}{\left(Cosh\alpha_1 h-Cos\beta_1 h\right)}$$

$$\lambda_{32}=\frac{Cot\varphi\left\{\mathrm{Sinh}\,\alpha_1 ySin\beta_1\left(y-h\right)-\mathrm{Sin}\,\beta_1 ySinh\alpha_1\left(y-h\right)\right\}+\left(Cosh\alpha_1 h-Cos\beta_1 h\right)}{\left(Cosh\alpha_1 h-Cos\beta_1 h\right)}$$

$$\lambda_{33}=\frac{M}{h_{ms}}\left\{\frac{Cot\varphi\left\{\mathrm{Sinh}\,\alpha_1 ySin\beta_1\left(y-h\right)+Sin\beta_1 ySinh\alpha_1\left(y-h\right)\right\}+\left(Cos\beta_1 h+Cosh\alpha_1 h\right)}{\left(\beta_1-\alpha_1 Cot\varphi\right)Sin\beta_1 h+\left(\alpha_1+\beta_1 Cot\varphi\right)Sinh\alpha_1 h}\right\}$$

$$\lambda_{34}=\frac{M}{h_{ms}}\left\{\frac{\mathrm{Cos}\,\beta_1 yCosh\alpha_1\left(y-h\right)+\mathrm{Cosh}\,\alpha_1 yCos\beta_1\left(y-h\right)}{\left(\beta_1-\alpha_1 Cot\varphi\right)Sin\beta_1 h+\left(\alpha_1+\beta_1 Cot\varphi\right)Sinh\alpha_1 h}\right\}$$